


# Urea transport B gene induces melanoma B16 cell death via activation of p53 and mitochondrial apoptosis

Lianqin Liu<sup>1</sup> | Yuxin Sun<sup>2</sup> | Yunxia Zhao<sup>1</sup> | Qian Wang<sup>1</sup> | Hua Guo<sup>1</sup> | Rui Guo<sup>1</sup> | Yanan Liu<sup>1</sup> | Shuang Fu<sup>3</sup> | Ling Zhang<sup>1</sup> | Yang Li<sup>1</sup> | Yan Meng<sup>1</sup> 

<sup>1</sup>Department of Pathophysiology, Prostate Diseases Prevention and Treatment Research Center, College of Basic Medical Science, Jilin University, Changchun, China

<sup>2</sup>Department of Otorhinolaryngology-Head and Neck Surgery, China-Japan Union Hospital, Jilin University, Changchun, China

<sup>3</sup>Department of Histology and Embryology, Changchun University of Traditional Chinese Medicine, Changchun, China

## Correspondence

Yang Li and Yan Meng, Department of Pathophysiology, Prostate Diseases Prevention and Treatment Research Center, College of Basic Medical Science, Jilin University, Changchun, China.  
Emails: lyang@jlu.edu.cn (YL); mengyan@jlu.edu.cn (YM)

## Funding information

The Science and Technology Natural Science Foundation of Jilin Provincial, Grant/Award Number: 20160101239JC; The National Natural Science Foundation of China, Grant/Award Number: 81370240, 81501982 and 81572927; The Health Technology Innovation Project of Jilin Province, Grant/Award Number: 2017J059

Urea Transporter B (UT-B) is a membrane channel protein that mediates the rapid transmembrane transport of urea and participates in urine concentration. Urea Transporter B is expressed in skin, but we found that there is little expression in human melanoma tissue. In this study, we examined the effects of UT-B overexpression in melanoma. The results indicated that there is no UT-B mRNA expression in B16 cells, and UT-B overexpression repressed B16 cell proliferation and induced apoptosis in vitro. We show that UT-B overexpression causes increased reactive oxygen species production, which may be caused by mitochondria dysfunction. The mitochondrial membrane potential ( $\Psi\Delta m$ ) was lower in UT-B-overexpressing B16 cells. The proteins involved in complexes I, III, IV and V of the respiratory chain were clearly downregulated in UT-B-overexpressing B16 cells, which would strongly reduce the activity of the electron transport chain. We found that mitochondrial release of cytochrome C into the cytoplasm also increased, indicating that apoptosis had been activated. In addition, UT-B overexpression reduced AKT phosphorylation and MDM2 expression and increased p53 expression; p53 activation may be involved in the anticancer effects of UT-B overexpression. Urea Transporter B overexpression also inhibited tumor growth in vivo. In conclusion, we demonstrated that UT-B may be related to the occurrence of melanoma and play a role in tumor development.

## KEYWORDS

B16 cells, mitochondrial apoptosis, p53, proliferation, UT-B

## 1 | INTRODUCTION

Melanoma is the most malignant skin tumor and is prone to distant metastasis. Current therapies include surgery, radiotherapy and chemotherapy, as well as small molecule therapeutics, such as BRAF V600 inhibitors, PD-1 monoclonal antibodies (mAbs), CTLA-4 mAb and MEK inhibitors.<sup>1</sup> However, many of these approaches result in side effects associated with drug resistance or immune-related effects after months of treatment. The overall occurrence of most cancer types tends to be stable or in decline, while both the incidence of

cutaneous melanoma and male mortality are on the rise.<sup>2</sup> Therefore, there is an urgent need for improved early diagnosis and treatment strategies for this cancer type.

Urea transporter B (UT-B) is encoded by the SLC14A1 (Slolute carrier family 14A gene) gene. The protein belongs to the solute carrier family. Urea transporter B is a transmembrane protein that specifically permeates urea, which mediates rapid urea transfer across the cell membrane driven by concentration differences. Urea transporter B transports urea 10-100 times faster than simple diffusion. Urea transporter B is widely expressed in the kidney, brain, heart,

This is an open access article under the terms of the Creative Commons Attribution-NonCommercial-NoDerivs License, which permits use and distribution in any medium, provided the original work is properly cited, the use is non-commercial and no modifications or adaptations are made.

© 2018 The Authors. *Cancer Science* published by John Wiley & Sons Australia, Ltd on behalf of Japanese Cancer Association.

liver and other tissues, and has certain physiological roles in these organs. Our early experiments found that UT-B knockout mice have a mitochondrial dysfunction in the heart.<sup>3</sup> Mitochondria play a central and multifunctional role in malignancy progression, and control redox balance, apoptosis and oncogenic signaling.<sup>4</sup> Targeted mitochondrial treatment methods can regulate the development of melanoma.<sup>5,6</sup> The expression of UT-B in bladder cancer was reported to be decreased and reduced further with tumor deterioration.<sup>7</sup> We are interested in whether there is such a phenomenon in melanoma and if UT-B can affect cancer cells through interference with mitochondrial function.

The literature has reported the expression of UT-B in the skin.<sup>8</sup> However, we found that UT-B expression was reduced or was absent in melanoma cell lines and melanoma tissues. This relationship suggests that UT-B may be related to the occurrence and development of melanoma. However, the mechanism by which UT-B is involved in melanoma is unclear.

*TP53* is a tumor suppressor gene whose activation induces cell cycle arrest and apoptotic cell death. *SIRT1* small molecule inhibitors reduce the proliferation and survival of human melanoma by activating p53.<sup>9</sup> Furthermore, bladder tissue of UT-B knockout mice underwent mitochondrial dysfunction and p53-dependent DNA damage and apoptosis.<sup>10</sup> However, there is no information on the UT-B regulatory mechanism in p53-dependent mitochondrial signaling to date.

In this study, we found that UT-B overexpression plays a role in tumor growth regulation in melanoma cell lines and mouse transplantation models, and this, combined with findings from UT-B inhibition in bladder cancer, suggests that UT-B may have tumor suppressor functions. We also analyzed the effect of UT-B on mitochondrial signaling in melanoma cells and elucidated the possible molecular mechanism. In summary, UT-B overexpression could be useful in the clinical treatment of cancer.

## 2 | MATERIALS AND METHODS

### 2.1 | Human melanoma

In this study, 4 melanoma patients were recruited from the Third Affiliated Hospital of Jilin University. The patients were aged between 58 and 78. Patients No. 1, No. 2 and No. 4 now survive, and No. 3 has died. The melanomas of these patients were all detected in primary organs and had no metastases. The melanomas of Patients No. 1 and No. 3 had crossed the dermis reticular layer and infringed upon the subcutaneous fat layer. According to Clark's analysis, the melanomas of Patients No. 1 and No. 3 were level 5. Melanomas of Patients No. 2 and No. 4 had infiltrated upon the dermis reticular layer. According to Clark's analysis, the melanomas of Patients No. 2 and No. 4 were level 4. Tumor tissue was obtained from operation specimens and preserved at  $-80^{\circ}\text{C}$  until use. This research was approved by the Human Research Ethics Committee of The Third Affiliated Hospital, College of Medicine, Jilin University. All 4 patients provided informed written informed consent.

### 2.2 | Cell culture

B16 melanoma cells were purchased from the Type Culture Collection of the Chinese Academy of Sciences (Shanghai, China). B16 cells were cultured in RPMI 1640, supplemented with 10% FBS (Clark, Logan, Utah, USA), and 1% penicillin G and streptomycin sulfate (Sigma, St. Louis, MO, USA). Cells were grown in a  $37^{\circ}\text{C}$  incubator supplied with 5%  $\text{CO}_2$ . In this study, cells were seeded into culture plates and transient transfections were performed the following day once cell confluency had reached 70%. After 48 hours of transfection, RNA and protein were extracted and used in subsequent experiments.

### 2.3 | Transient transfection

B16 cells were transfected with control plasmid (pcDNA3.1) or overexpression plasmid (pcDNA3.1-UT-B). Both pcDNA3.1 and pcDNA3.1-UT-B were purchased from Shanghai GenePharma (Shanghai, China). Prior to transfection, cells were cultured in 96-well plates, 24-well plates or 6-well plates until they had reached 70% confluency. The thermo transfection agent Interferin (Thermo Fisher Scientific, Waltham, MA, USA) was used according to the manufacturer's protocol. After transfection for 48 hours, cells were collected for subsequent analysis.

### 2.4 | RT-PCR analysis

Total RNA lysate was extracted from tissue samples or cell lines using Trizol (Invitrogen, Carlsbad, CA, USA) based on standard protocols, and cDNA synthesis was performed using a Super RT Kit (BioTeke, Beijing, China) following the manufacturer's protocol with the following primers:

UT-B forward: 5'-AATGTTTCATGGCGCTCACCT-3', and reverse: 5'-ACAAGCTGGCAATCCAACCT-3'

GAPDH primers used for the human tissues:

Forward: 5'-TGGTATCGTGAAGGACTCATGAC-3'

Reverse: 5'-TGCCAGTGAGCTTCCCGTTCAGC-3'

GAPDH primers used for the B16 cells:

Forward: 5'-AGAAGGCTGGGGCTCATTTG-3'

Reverse: 5'-AGGGCCATCCACAGTCTTC-3'

### 2.5 | MTT assay

B16 cells were inoculated in 96-well plates at a concentration of  $4 \times 10^3$  cells/well for transfection experiments. PU14 is a novel inhibitor of human and mouse UT-B, which is effective in inhibiting UT-B activity.<sup>11</sup> The UT-B inhibitor PU14 group (U+ PU14) was added with 2, 4 and 6  $\mu\text{mol/L}$  PU14 at the same time as transfection. After 24, 48 and 72 hours of transfection, 10  $\mu\text{L}$  MTT was added and plates were incubated for 4 hours. Absorbance was measured at 570 nm using a microplate reader (FLUOstar Omega, Offenburg, Germany).

### 2.6 | Clonogenic capacity

Harvested cells were suspended in culture liquid and seeded in 6-well plates at a concentration of 300 cells/well. ZVAD (caspase inhibitor)

was purchased from Selleckchem. ZVAD is a caspase inhibitor that inhibits apoptosis.<sup>12</sup> In the experiment, 20  $\mu\text{M}$  ZVAD was added to the cell culture medium, and the plasmid was transfected half an hour later. Apoptosis was detected by flow cytometry or Hoechst after 48 hours. After 10 days, the culture medium was discarded and cells were fixed with 4% paraformaldehyde for 30 minutes. Finally, cells were Giemsa-stained and photographed.

## 2.7 | Assessment of cell apoptosis

Six-well plates were seeded with B16 cells at a concentration of  $4 \times 10^5$  cells/well. Transfection experiments were performed the following day. Cells were collected after 48 hours and washed twice with PBS. B16 cells were resuspended in 1 $\times$  buffer, then 5  $\mu\text{L}$  Annexin V-FITC and 5  $\mu\text{L}$  PI (50  $\mu\text{g}/\text{mL}$ ) (FITC Annexin V Apoptosis Detection Kit, BD Biosciences, San Jose, CA, USA) were added and plates were incubated in the dark at room temperature for 15 minutes. Then, 400  $\mu\text{L}$  of 1 $\times$  buffer was added to each sample. The stained cells were then rinsed twice with serum-free RPMI 1640, and fresh serum-free RPMI 1640 was added. Finally, flow cytometry (BD FACSCalibur, San Jose, CA, USA) was performed to detect apoptosis.

## 2.8 | Hoechst 33258 staining

Forty-eight hours after B16 cells were transfected in 24-well plates, the cells were fixed with 4% paraformaldehyde for 5 minutes. B16 cells were then stained with 1 mg/mL Hoechst (Beyotime Biotechnology, Nantong, China) for 10 minutes at room temperature in the dark. Finally, the cells were washed twice with PBS and immediately imaged by fluorescence microscopy.

## 2.9 | Measurement of mitochondrial membrane potential

B16 cells were harvested 48 hours after transfection and then resuspended in 1 mL of JC-1 (5  $\mu\text{g}/\text{mL}$ , Beyotime Biotechnology) and incubated for 30 minutes. Then, cells were washed twice with serum-free medium and resuspended in serum-free medium. Finally, flow cytometry (FACSCalibur) was used to detect mitochondrial membrane potential.

## 2.10 | Measurement of intracellular reactive oxygen species levels

Harvested cells were suspended in 100  $\mu\text{L}$  RPMI 1640 without FBS and were then incubated with DCFH-DA fluorescent probe for 20 minutes. Intracellular reactive oxygen species (ROS) was detected by flow cytometry (FACSCalibur). DCFH-DA itself has no fluorescence and can pass through the cell membrane freely. After DCFH-DA enters the cell, it is hydrolyzed by intracellular color esterase to generate DCFH. Intracellular ROS can oxidize fluorescent DCFH to produce fluorescent DCF. The level of ROS in the cell can be analyzed by measuring the fluorescence of DCF.

Forty-eight hours after B16 cells were transfected in 24-well plates, the medium was removed and the diluted DCFH-DA (10  $\mu\text{mol}/\text{L}$ ) was added. The cells were then incubated with DCFH-DA fluorescent probe for 20 minutes. The images were viewed and recorded with a fluorescence microscope (Olympus, Japan).

## 2.11 | Immunofluorescence analysis

Urea transporter B expression was observed by immunostaining and imaging. After transfection with pcDNA3.1 or pcDNA3.1-UT-B for 48 hours, cells were seeded on coverslips placed in a 24-well plate and fixed with 4% paraformaldehyde after 24 hours. After 30 minutes, cells were washed with 1 $\times$  PBS and blocked with BSA (Sigma) for 2 hours at room temperature. Cells were incubated with primary antibodies against UT-B (1:400; Santa Cruz Biotechnology, Santa Cruz, CA, USA) for 20 hours, and then incubated with Alexa Fluor-conjugated secondary antibodies (1:1000; Invitrogen/Thermo Fisher Scientific) and DAPI (Solarbio, Beijing, China) for 5 minutes in the dark at room temperature. The images were viewed and recorded with a fluorescence microscope (Olympus, Japan).

## 2.12 | Immunofluorescent staining

Sections were washed with PBS for 5 minutes and then fixed in 4% paraformaldehyde for 10 min at room temperature. All washes ( $3 \times 10$  minutes) between stages were performed in PBS. After the sections had been permeabilized with .2% Triton X-100 (Sigma) in PBS for 5 minutes, potential non-specific binding sites were blocked with antibody dilution buffer (2% goat serum [Sigma] and 1% IgG-free BSA [Sigma] in PBS) for 20 minutes at room temperature. Sections were then incubated with UT-B antibodies (1:400, Santa Cruz Biotechnology) overnight at 4°C. After washing, the sections were then incubated with secondary antibodies for 1 hour at room temperature. Following the final washing step, the glass coverslips were mounted upside down on clean microscope slides with Fluorescence Mounting Medium (DAKO).

## 2.13 | Western blot analysis

B16 cells were harvested and washed with cold PBS. Cells and tumor tissue were lysed in RIPA Buffer (Boston BioProducts, Ashland, MA, USA) containing protease inhibitors (Sigma). The supernatant was obtained by centrifugation at 15 000 g for 20 minutes at 4°C. Protein concentration was determined using the BCA Protein Assay Kit (Thermo Fisher Scientific). We loaded the loading buffer and boiled the mixture for 10 minutes. Total protein extract (300  $\mu\text{g}$ ) was used for immunoblot analysis. The same amount of protein sample (30  $\mu\text{g}$ ) was separated by 12% SDS-PAGE gel and transferred to PVDF membrane (Millipore, Billerica, MA, USA). Membranes were blocked in blocking solution (non-fat milk in 1 $\times$  TBST) for 1 hour at room temperature and incubated with the primary antibody at an appropriate concentration overnight at 4°C. The membrane was washed 3 times with TBST and Western Lightning-ECL from Pierce

ECL Western Blotting Substrate (Thermo Fisher Scientific) for detection. The following primary antibodies were used in this study: anti-BCL2 (Cell Signaling Technology CST, Danvers, MA, USA; product number 60178-1), anti-BAX (Cell Signaling Technology CST, Danvers, MA, USA; product number 50599-2), anti-MDM2 (Proteintech Group, Wuhan, China; product number 19058-1), anti-p53 (Proteintech Group, Wuhan, China; product number 10442-1),  $\beta$ -actin (Proteintech Group, Wuhan, China; product number 66009-1), anti-p21 (Proteintech Group, Wuhan, China; product number 10355-1), anti-phospho-AKT (Arigo, Taiwan; product number ARG51559) and anti-UT-B (Santa Cruz Biotechnology). The primary antibodies used in this study were: anti-NDUFV1, anti-CYC1, anti-COX7C, anti-SOD2, anti-HSP60, anti-ATP5F1 and anti-COXIV (Proteintech Group, Wuhan, China; product numbers: 11238-1, 10242-1, 11411-2, 24127-1, 15282-1, 15999-1 and 11242-1).  $\beta$ -actin used as an endogenous control and COXIV as mitochondrial control. The density of the bands was analyzed using image analysis software (IMAGE J).

## 2.14 | Isolation of the mitochondria

Mitochondrial proteins were extracted using a cell mitochondrial separation kit (Beyotime Biotechnology). B16 cells were transfected with pcDNA3.1 and pcDNA3.1-UT-B, and  $5 \times 10^7$  cells were collected after 48 hours. Next, 1 mL of a mixture of separation reagent and PMSF (1 mmol/L) was added to 50 million cells, which were gently mixed and left in an ice bath for 10-15 minutes. The cell suspension was transferred to a suitable sized glass homogenizer and homogenized. Then, 2  $\mu$ L of the cell homogenate was taken, and 30-50  $\mu$ L trypan blue staining solution was added. After mixing, the proportion of trypan blue-stained cells was observed under a microscope. When the staining ratio reached 50%, the cells were homogenized at 600 g for 10 minutes at 4°C. The supernatant was then carefully transferred to another centrifuge tube and centrifuged at 11 000 g for 10 minutes at 4°C to precipitate cellular mitochondria. The supernatant was then collected and centrifuged at 12 000 g for 10 minutes at 4°C to separate the mitochondrial cytoplasmic protein. Next, 150  $\mu$ L of PMSF was added to the mitochondria. After incubation on ice for 30 minutes, the lysate was centrifuged at 12 000 g for 10 minutes at 4°C to obtain mitochondrial protein.

## 2.15 | Oxygen consumption rate extracellular acidification rate

The oxygen consumption rate (OCR) and extracellular acidification rate (ECAR) assay kits were MitoXpress Xtra and pH-Xtra assay kits, purchased from Luxcel Biosciences (Cork, Ireland). We examined the oxygen consumption and glycolysis of transfected B16 cells according to the instructions.

## 2.16 | Animal experiments

*Salmonella typhimurium* A1-R (*S. typhimurium* A1-R) attenuated by leu and arg auxotrophy has been shown to target multiple types of

cancer in mouse models.<sup>13</sup> We used the Gene Pulser Transfection Apparatus (Bio-Rad, 1652100, California, USA) to transfer plasmids into competent attenuated *S. typhimurium*. The instructions indicated that the electrophoretic conditions for attenuated *S. typhimurium* were the same as for *E. coli*, so we performed the test according to section 6.1 (*E. coli*) in the instructions. After many tests, we concluded that the optimal condition for the electrotransfer of attenuated *Salmonella* is 2.5 KV and 25  $\mu$ F. We introduced plasmid into attenuated *S. typhimurium* (PQ) by electrical transfection method to generate PQ-UT-B bacteria (PQ-U) for subsequent experiments. At the same time, the control group was transfected with the empty plasmid pcDNA3.1.

This animal study was approved by the Animal Ethics Review Committee of Basic Medical Sciences, Jilin University in accordance with the regulations of the Institutional Committee for the Care and Use of Laboratory Animals of the Experimental Animal Center of Jilin University. Mice were housed under a 12/12 hour light/dark cycle in an air-conditioned room at  $22 \pm 2^\circ\text{C}$  with free access to food and water. Eleven-week-old C57 male mice were purchased from the Beijing Academy of Medical Sciences Animal Research Center. A total of 18 mice, each weighing 18-22 g, was used. Each mouse was injected with 100  $\mu$ L cell suspension containing  $3 \times 10^6$  B16 cells. The route of injection of B16 cells into mice is subcutaneous injection. When the tumor size was 3-5 mm, the mice were divided into 3 groups. Mice were injected through the tail vein with  $5 \times 10^6$  cfu of PQ, PQ-pcDNA3.1 or PQ-UT-B. We measured tumor size and mouse weight every other day. Tumor size was measured by calipers, and tumor volume was calculated using the following formula:  $V = (\text{length})^2 \times (\text{width})/2$ . After tumor injection for 14 days, mice were killed by intraperitoneal administration of an anesthetic drug cocktail (240 mg/kg) followed by cervical dislocation. Tumor tissue was removed for subsequent testing. Each tumor tissue was divided into 2 parts: 1 part was frozen at  $-80^\circ\text{C}$  degrees for protein and RNA extraction, and the other part was fixed in 4% paraformaldehyde for immunofluorescent staining.

## 2.17 | Statistical analysis

All the presented data were confirmed in a minimum of 3 independent experiments and expressed as the mean  $\pm$  SD. Statistical analyses were performed using SPSS version 17.0. One-way ANOVA followed by the Newman-Keuls test was used to compare the differences between pcDNA3.1 and pcDNA3.1-UT-B.  $P < .05$  was considered to indicate a statistically significant difference.

# 3 | RESULTS

## 3.1 | Urea transporter B expression in human melanoma tissue

To investigate the differences in UT-B expression in skin tumors, we obtained cancer tissue from 4 melanoma patients. Melanoma tissue

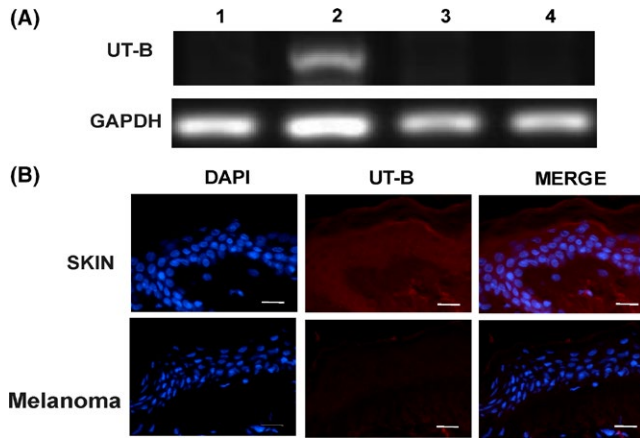


**FIGURE 1** Urea transporter B (UT-B) expression in human melanoma. Three of four tissue samples did not express UT-B. A, The numbers represent 4 different melanoma tissues from 4 different melanoma patients. B, Immunofluorescence experiments were performed on normal human skin and tumors using anti-UT-B antibodies and cell nucleus marker DAPI. Blue: DAPI staining; red: UT-B protein staining. Scale bar = 10  $\mu$ m

was lysed, and extracts were subjected to RT-PCR. Three samples did not express UT-B (Figure 1A), and immunostaining of normal human skin and patients' melanoma tissue showed that UT-B was expressed in the normal skin, while UT-B expression was weak in tumors (Figure 1B). The expression of UT-B has been reported in the skin,<sup>8</sup> inferring that UT-B levels may be related to the development of melanoma. Thus, the next step was to study whether UT-B has an effect on melanoma.

### 3.2 | Urea transporter B overexpression repressed cell proliferation, clonogenic capacity and migration of B16 cells

We selected UT-B non-expressing B16 cells and transfected them with pcDNA3.1 and pcDNA3.1-UT-B to study the effect of UT-B on melanoma that does not express UT-B. To assess the validity of our model system, we first investigated mRNA and protein levels upon pcDNA3.1-UT-B transfection. B16 cells transfected with pcDNA3.1-UT-B were lysed at 48 h after transfection, and extracts

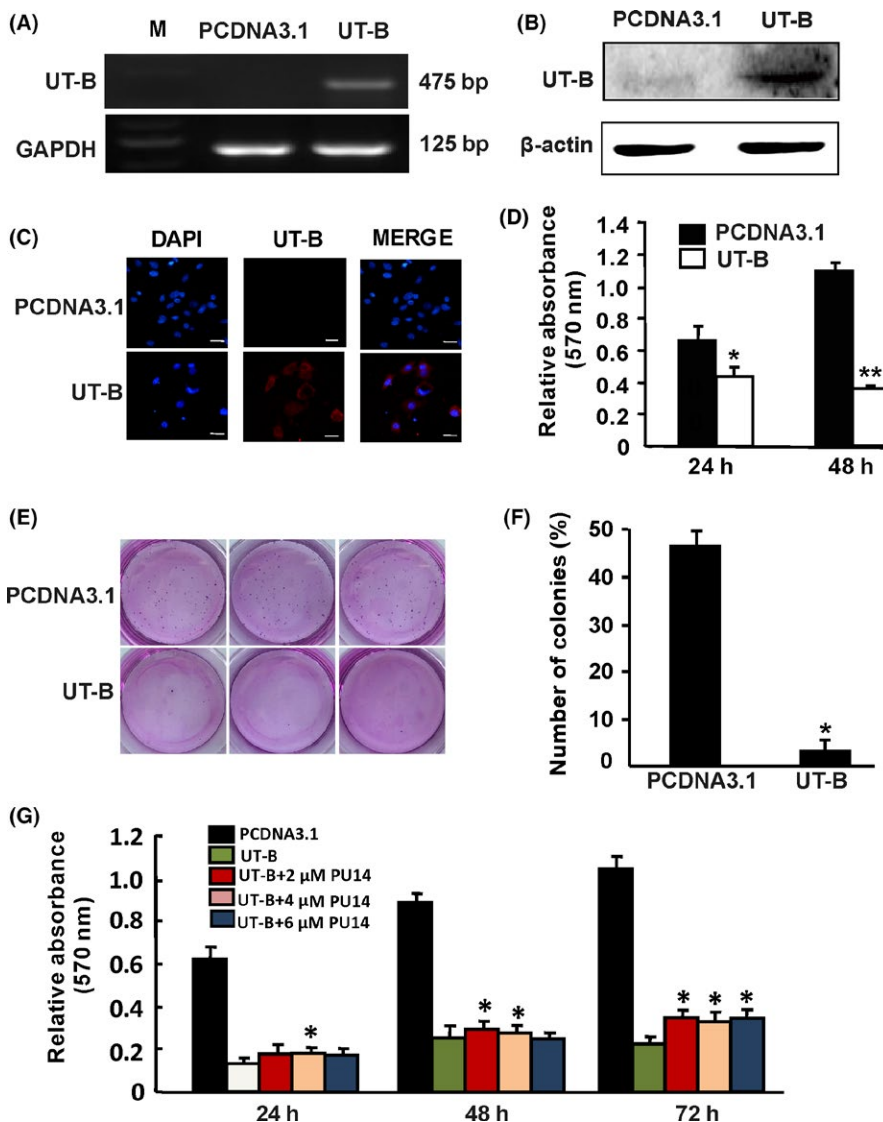


**FIGURE 2** Urea transporter B (UT-B) overexpression represses cell proliferation and clonogenic capacity of B16 cells. (A) mRNA levels and (B) protein levels of UT-B at 48 hours post-transfection and densitometric quantification of proteins normalized to  $\beta$ -actin. C, B16 cells seeded onto chamber slides were transfected with pcDNA3.1-UT-B for 48 hours and immunofluorescent staining was performed using anti-UT-B antibodies and cell nucleus marker DAPI. Blue: DAPI staining; red: UT-B protein staining. Scale bar = 10  $\mu$ m. D, MTT cell viability in B16 cells. B16 cell proliferation after 24 and 48 h transfection as measured by MTT assay. E, Colonies generated after 10 days of incubation in methylcellulose-based medium. F, Graphs with quantitative data for the colony formation assay, respectively. G, The MTT assay detects the effect of the UT-B inhibitor PU14 on overexpression of UT-B cells. \* $P < .05$ , \*\* $P < .01$  vs pcDNA3.1 group or U+PU14 group



were subjected to RT-PCR and western blot analysis. As shown in Figure 2A,B, the mRNA and protein levels of UT-B in B16 cells were significantly increased after transfection compared with B16 cells transfected with the control vector (pcDNA3.1). Immunostaining of B16 cells transfected with pcDNA3.1-UT-B over for 48 hours showed an increase in UT-B in the cytoplasm and cell membrane (Figure 2C). Cell viability was detected by MTT assay. After UT-B was overexpressed in B16 cells, cell proliferation was decreased by 31.5% and 67.6% at 24 and 48 hours, respectively (Figure 2D). In addition, we performed colony formation assays to determine whether overexpression of UT-B impaired the clonogenic capability of B16 cells (Figure 2E,F). The number of colonies generated from individual cells was drastically reduced in UT-B-transfected B16 cells. To further confirm the inhibitory effect of UT-B on B16 cells, UT-B inhibitor PU14<sup>41</sup> was added while transfecting UT-B-PC-DNA3.1.

Overexpression of UT-B with the addition of UT-B inhibitors can attenuate UT-B-induced apoptosis to some extent (Figure 2G). Overexpression of UT-B may cause irreversible damage to the cells, so the addition of the inhibitor did not completely rescue cell survival, which may also be related to the fact that the inhibitor does not completely inhibit UT-B function. These data, together with the results from Figure 2, suggested that UT-B plays an inhibitory role in cell proliferation and clonogenic capacity of B16 cells.

### 3.3 | Urea transporter B overexpression induced B16 cell apoptosis

To investigate the mechanism of UT-B overexpression in B16 cells, we detected apoptosis in cells transfected with pcDNA3.1-UT-B for 48 hours by flow cytometry, demonstrating that apoptotic cell

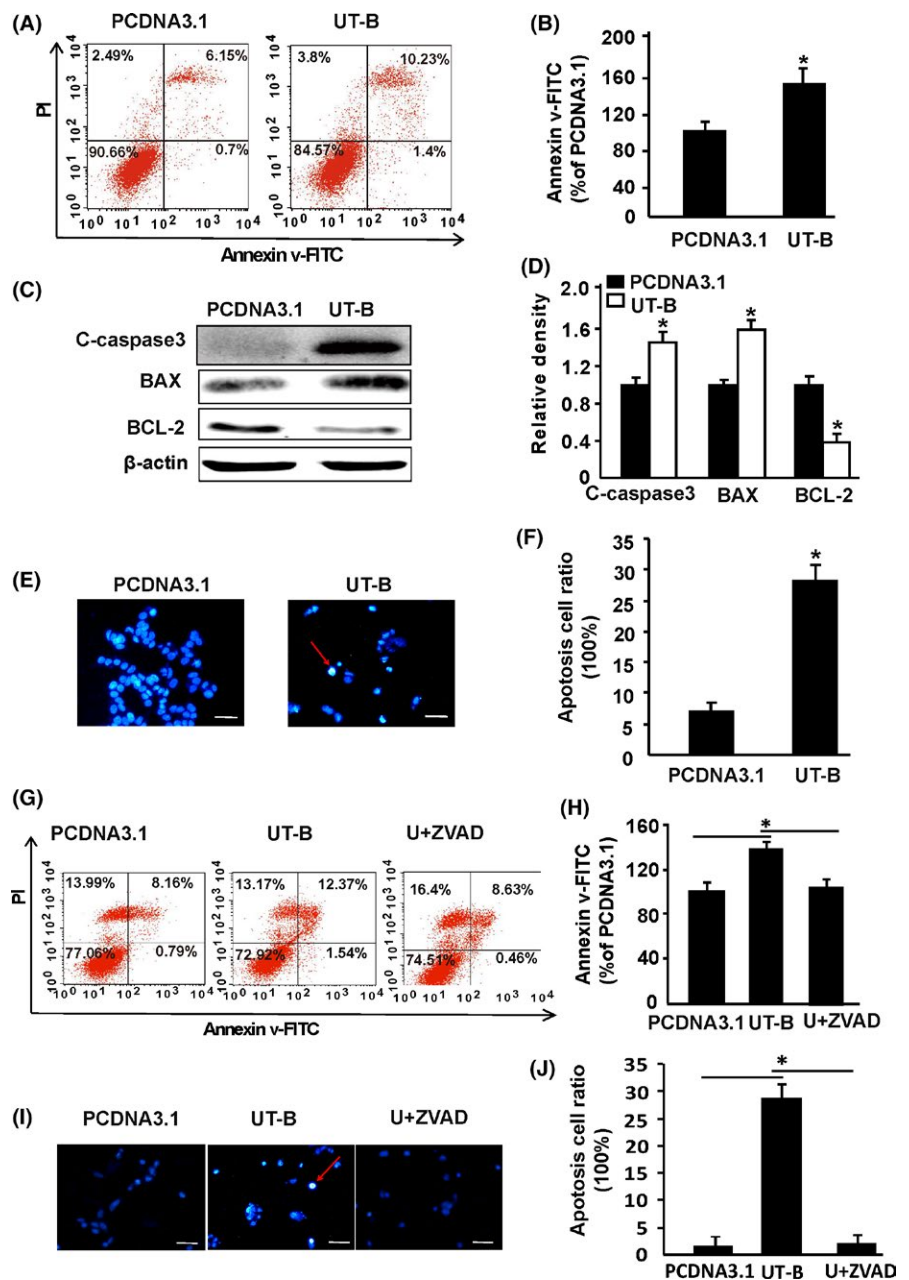


**FIGURE 3** Urea transporter B (UT-B) overexpression induces apoptosis. A, B, FITC Annexin V/PI staining indicated increased apoptosis. C, D, BCL-2 levels were reduced, and BAX and cleaved caspase-3 were increased in transfected B16 cells. E, I, Morphological changes in the nuclei were examined by Hoechst 33258 staining and fluorescence imaging. F, J, The percentage graph of apoptotic cell. G, H, FITC Annexin V/PI staining indicated that the apoptosis inhibitor ZVAD can inhibit the apoptosis of overexpressing UT-B cells. Scale bar: 10  $\mu$ m. n = 3, \*P < .05 vs pcDNA3.1 group or U+ZVAD group

numbers were increased (Figure 3A,B). Meanwhile, western blotting showed that the expression of apoptotic proteins cleaved caspase-3 and BAX was increased, and the expression of BCL-2 was decreased (Figure 3C,D). Hoechst staining showed that after transfection with pcDNA3.1-UT-B, the number of cells undergoing apoptosis was increased (Figure 3E,F). In Figure 3E, the red arrow points to the apoptotic cell. The caspase inhibitor ZVAD was added half an hour before overexpression of UT-B in B16 cells. Flow cytometry and Hoechst results showed that ZVAD attenuated UT-B-induced B16 cell death and did not completely rescue cell death (Figure 3G-J), suggesting that overexpression of UT-B may induce cell death through the apoptotic pathway, and may also induce cell death through other pathways.

### 3.4 | Urea transporter B overexpression increased intracellular reactive oxygen species and reduced mitochondrial membrane potential in B16 cells

Reactive oxygen species accumulation of cells induces cytotoxicity, so we next investigated whether intracellular ROS changes following UT-B overexpression. Using flow cytometry to detect DCFH-DA fluorescent probe, we demonstrated that ROS was significantly increased following transfection with pcDNA3.1-UT-B compared with the control group (Figure 4A,B). ROS fluorescence assay also showed an increase in ROS production after overexpression of UT-B in B16 cells (Figure 4E). We examined mitochondrial membrane potential using JC-1, a mitochondria-specific

fluorescent probe that exhibits potential-dependent accumulation in mitochondria with a concomitant shift in the peak of emission spectrum from green ( $\approx 529$  nm) to red ( $\approx 590$  nm). At the same time, mitochondrial membrane potential was found to be reduced (Figure 4C,D). A preliminary explanation is that mitochondrial function was decreased after transfection with pcDNA3.1-UT-B.

### 3.5 | Urea transporter B overexpression attenuated mitochondrial function and affected the metabolism

Mitochondrial dysfunction plays an important role in carcinogenesis and the effects of downstream pro-apoptotic proteins.<sup>14</sup> To further study the changes in mitochondrial function after transfection with pcDNA3.1-UT-B, we analyzed oxygen-free radical scavenging enzymes representing complexes I, III, IV and V of the mitochondrial respiratory chain, NDUFV1, CYC1, COX7C and ATP5F1, respectively, and superoxide dismutase 2 (SOD2), by western blotting. The results showed that NDUFV1, CYC1, COX7C and ATP5F1 expression was downregulated after transfection with pcDNA3.1-UT-B (Figure 5A,B). The expression of HSP60 and SOD2 was also downregulated (Figure 5C,E). These results indicate that after transfection with pcDNA3.1-UT-B, B16 cells lack mitochondrial complex subunits and have disordered electron transfer, which may account for the increase in ROS and the reduced mitochondrial membrane potential. In addition, it has been shown that some of the stress signals mediated and regulated by BCL-2 family proteins result in mitochondria releasing cytochrome c.<sup>15</sup> This is, indeed, the first step

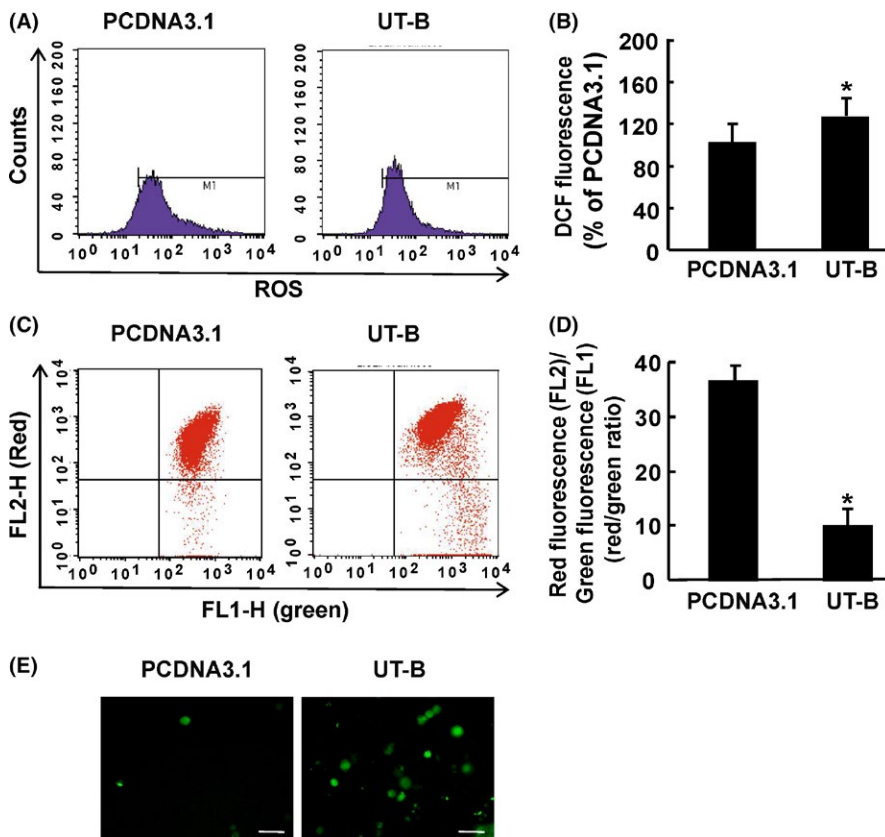


**FIGURE 4** Generation of intracellular reactive oxygen species (ROS) and mitochondrial membrane potential ( $\Delta\Psi_m$ ). (A, B) ROS was increased and (C, D) mitochondrial membrane potential was decreased in B16 cells after transfection for 48 h. Indicated mitochondrial oxidative phosphorylation dysfunction and ATP insufficiency in the transfected B16 cells. E, The amount of ROS produced in the cells was observed under a microscope. \* $P < .05$  vs pcDNA3.1 group

in the intrinsic pathway of apoptosis.<sup>16</sup> Figure 3 shows that after transfection with pcDNA3.1-UT-B, the expression of BCL-2 protein was decreased and the expression of BAX protein was increased. In addition, the results showed that the expression of CYC1 cytoplasmic protein was increased (Figure 5D,F), indicating that the mitochondrial membrane potential may be reduced. These results suggest that the release of CYC1 from the mitochondria to the cytoplasm after transfection with pcDNA3.1-UT-B initiates the mitochondrial apoptotic pathway to induce cell death. To determine mitochondrial function, we examined the mitochondrial OCR and

found that it was significantly decreased in B16 cells transfected with pcDNA3.1-UT-B (Figure 5G), further confirming mitochondrial dysfunction. In B16 cells, after overexpression of UT-B, the expression of the glucose transporter GLUT1 was decreased and glucose uptake was reduced (Figure 5I,J,K). Decreased OCR indicates a decrease in oxygen consumption and a decrease in aerobic respiration (Figure 5G). ECAR decreased (Figure 5H), indicating that lactic acid production was reduced and glycolysis was weakened. The expression of the mRNA of the fat synthesis key FASN and SREBP1 is reduced (Figure 5L). In conclusion, overexpression of UT-B in B16 cells

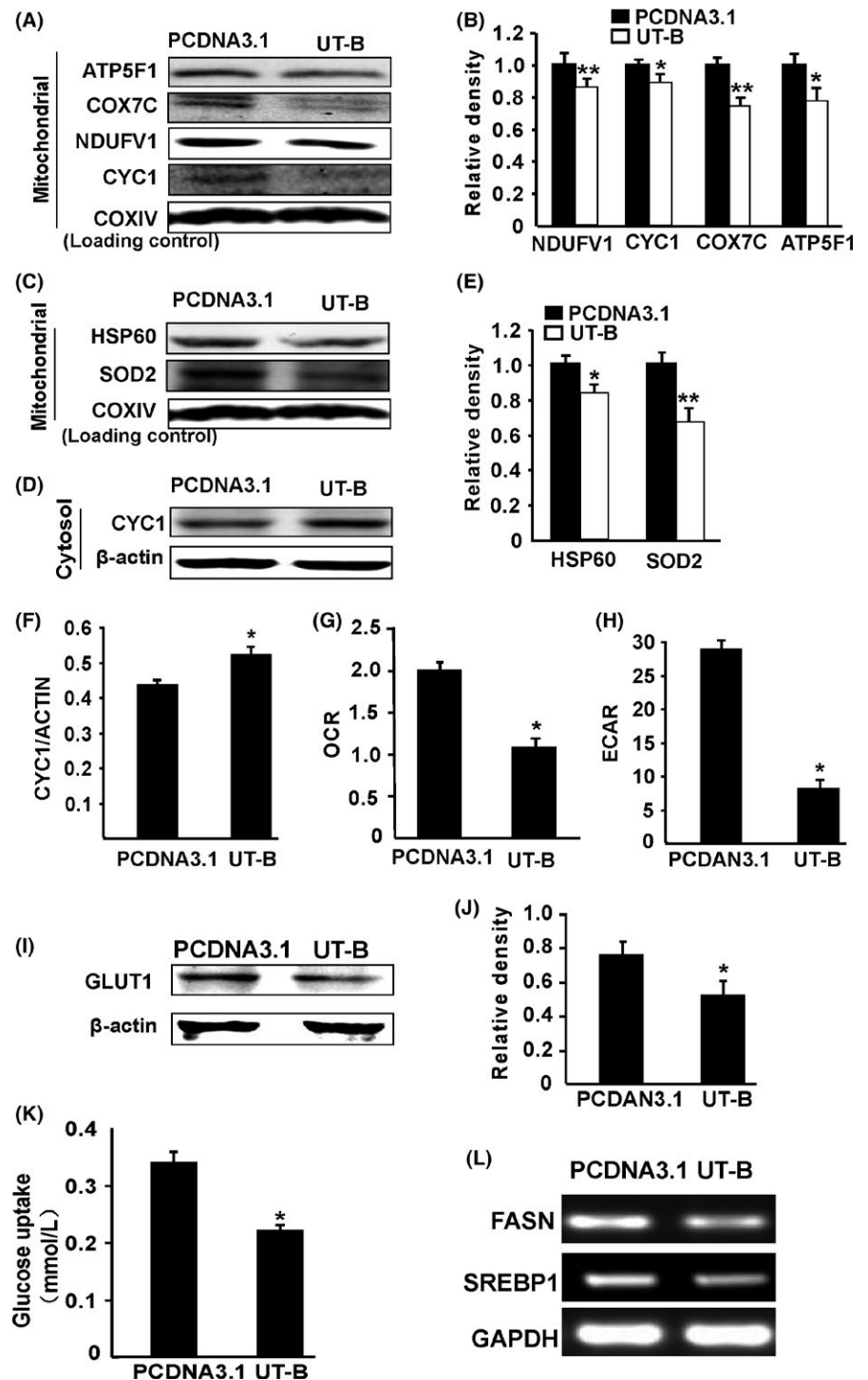


**FIGURE 5** Mitochondrial protein changes in transfected B16 cells. A, NDUFV1, CYC1, COX7C and ATP5F1 were reduced in the transfected B16 cell mitochondria. C, Enzymes that scavenge reactive oxygen species (SOD2) and important functional proteins (HSP60) in the mitochondria were downregulated in the mitochondria of the transfected B16 cells. D, CYC1 was upregulated in the cytoplasm of the transfected B16 cells. B, E, F, Densitometric analysis of the protein bands. G, Oxygen consumption rate decreased after transfection with pcDNA3.1-UT-B. H, Extracellular acidification rate decreased after transfection with pcDNA3.1-UT-B. I, J, GLUT1 protein levels were determined by western blot analysis. K, The amount of glucose uptake in the cells is reduced. L, RT-PCR experiments showed decreased expression of fat synthase FASN and SREBP1. \* $P < .05$ , \*\* $P < .01$  vs pcDNA3.1 group



affects cell metabolism. The above metabolic processes are carried out in mitochondria, and the effect of expressing UT-B on metabolism must be achieved by affecting the enzyme or protein function in the mitochondria. Conversely, these metabolic changes can also affect the function of mitochondria.

### 3.6 | Urea transporter B overexpression induced apoptosis through the p53 pathway

Studies show that many anti-cancer drugs can induce apoptosis in cancer cells through a variety of pathways, partly through the activation of p53.<sup>17-19</sup> We examined whether apoptosis of B16 cells transfected with pcDNA3.1-UT-B is associated with p53. Activated AKT enhances MDM2-mediated ubiquitination and p53 degradation.<sup>20</sup> We detected increased p53 expression in B16 cells transfected with pcDNA3.1-UT-B (Figure 6). Furthermore, we found that upstream P-AKT and MDM2 expression was decreased, and downstream p21 expression was increased (Figure 6). Therefore, transfection with pcDNA3.1-UT-B may result in p53 activation to promote apoptosis.

### 3.7 | Urea transporter B overexpression inhibited B16 tumor growth in vivo

To further study the effect of UT-B on B16 cells, we conducted an in vivo experiment. B16 xenograft mouse models were then used to determine the function of UT-B in vivo. We found that UT-B was expressed in mouse skin but not in the PQ group tumors (Figure 7A). Urea transporter B overexpression inhibited tumor growth in vivo (Figure 7B,C). PQ-U group tumor volume and weight were significantly reduced (Figure 7D,E). Urea transporter B expression was detected in PQ-U tumors (Figure 7F,G). Consistent with in vitro experiments, p-AKT, MDM2 and BCL-2 protein expression was decreased, and p53, p21 and BAX expression was increased in PQ-U tumors (Figure 7H). Furthermore, UT-B overexpression may induce B16 cell death by activating p53 and mitochondrial apoptosis. In animal experiments, the expression level of UT-B in mouse B16 tumors was significantly lower than that in mouse skin, which is consistent with the results of human tissue in Figure 1, indicating that UT-B expression changes during melanoma development, and UT-B may be involved in the development of melanoma. Both in vitro and in vivo experiments have shown that overexpression of UT-B in tumors inhibits tumor cell growth, so UT-B may play an important role in tumor development.

## 4 | DISCUSSION

To date, limited studies have shown that UT-B expression in bladder urothelial carcinoma cells is reduced or absent and that its expression is closely related to tumor grade and pathology. Low UT-B expression may be associated with the incidence, progression and aggressiveness of bladder urothelial carcinoma.<sup>7</sup> Urea transporter B is expressed in normal skin,<sup>8</sup> but we found that it was absent in B16

melanoma cells. Therefore, we hypothesized that UT-B expression may be associated with melanoma progression.

To study the role of the UT-B in the development and progression of melanoma, we overexpressed UT-B in B16 cells. After transfection with pcDNA3.1-UT-B, the proliferation, migration and clonogenic capacity of B16 cells were decreased and apoptosis was increased.

Urea transporter B is a membrane channel protein that is involved in the transmembrane transport of urea following the urea gradient. Urea is the final product of protein metabolism. Changing the expression of UT-B on the membrane will affect the instantaneous concentration of urea inside and outside the cell, thereby affecting cell energy metabolism. In B16 cells, after transfection of the UT-B-PC-DAN3.1 plasmid, the expression level of UT-B in B16 cells was increased. Urea in the cell may flow out of the cell through UT-B, promoting urea circulation. It has been reported in the literature that inhibition of the urea cycle allows more aspartic acid to be used in pyrimidine synthesis and promotes tumor cell proliferation.<sup>21</sup> Aspartic acid produced by glucose metabolism in tumor cells is used in the urea cycle, and citric acid produced by glucose metabolism is related to lipid metabolism. Arginine is produced by 2 urea cycles, and arginine changes in melanoma affect glucose metabolism and lipid metabolism.<sup>22</sup> Therefore, we suspect that overexpression of UT-B in B16 cells changes the instantaneous concentration of urea, affecting the relevant urea cycle, which, in turn, affects glucose metabolism and lipid metabolism. Metabolic reprogramming is the energy basis of cancer cell proliferation and metastasis. We are the first to report that when UT-B-expressing skin cells are transformed into melanoma cells, UT-B expression is decreased or completely absent; this change may be one of the requirements of tumor cell metabolism reprogramming and unrestricted proliferation. Therefore, in this study, re-expression of UT-B in melanoma B16 cells affected the proliferation of tumor cells, possibly through urea-related metabolism.

After transfection with pcDNA3.1-UT-B, the mitochondrial membrane potential of B16 cells was also decreased, revealing mitochondrial dysfunction in these cells. The expression of NDUFB1, CYC1, COX7C and ATP5F1, which represent mitochondrial complexes I, III, IV and V, respectively, is decreased, and OCR was decreased, further indicating that mitochondrial function was impaired. In cardiac

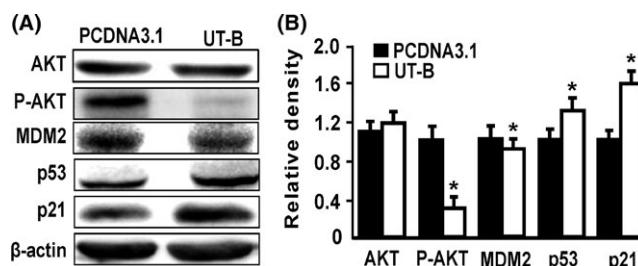


**FIGURE 6** Changes in P-AKT/p53 protein levels after transfection with pcDNA3.1-UT-B. A, AKT, P-AKT, p53, MDM2 and p21 protein levels were determined by western blot analysis. B, Densitometric analysis of protein bands. \* $P < .05$  vs pcDNA3.1 group

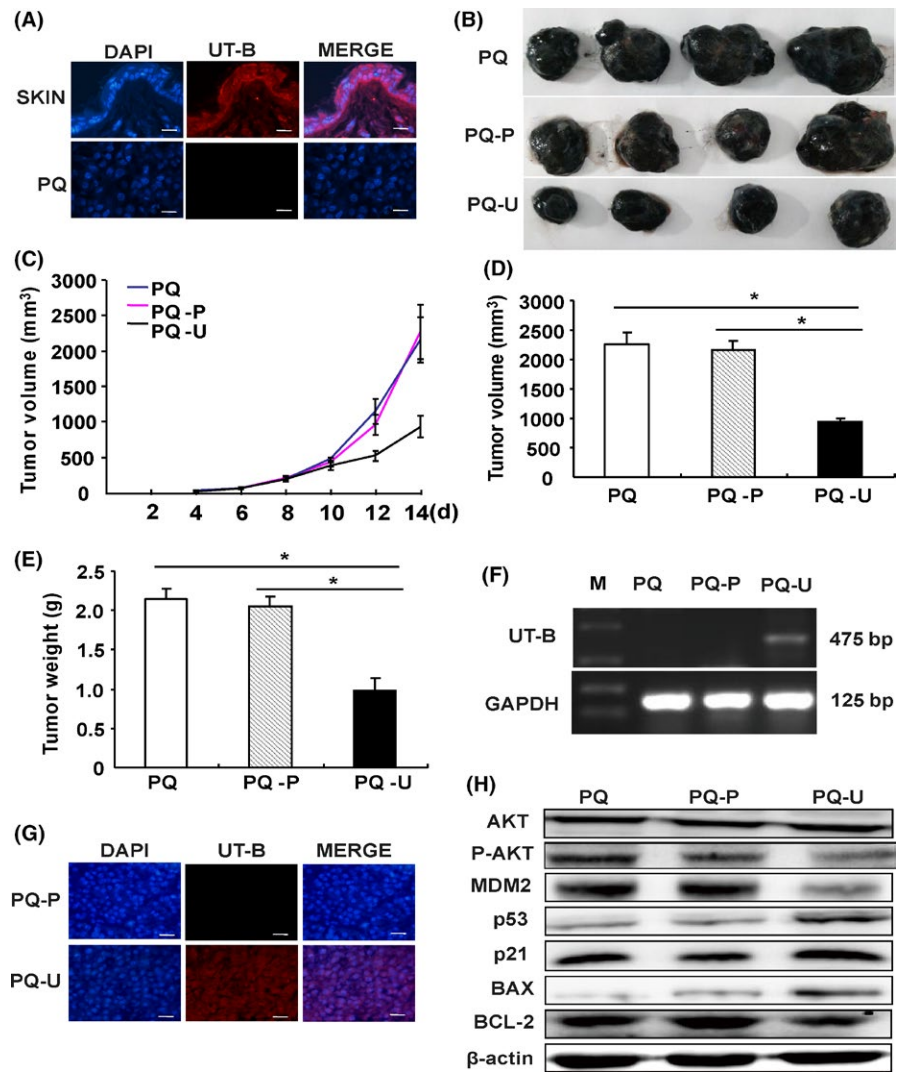


**FIGURE 7** Urea transporter B (UT-B) overexpression inhibited tumor growth and reduced tumor volume in vivo. B16 cells were injected into C57 mice 5 days before treatment with PQ/PQ-pcDNA3.1 (PQ-P)/PQ-UT-B (PQ-U). A, Immunofluorescent staining showing that differences in UT-B expression between skin and B16 tumor transfected with pcDNA3.1. B, Image of the tumor tissues for each treatment group. C, Tumor growth inhibition in C57 mice bearing B16 tumors after tail vein injection of different formulations. (D) Comparison of the tumor volume and (E) weight of PQ-U group vs PQ and PQ-P group ( $n = 4$ ). (F) PCR assay and (G) immunofluorescent staining verified B16 tumor expressing UT-B gene after treatment with PQ-U. H, AKT, p-AKT, p53, MDM2, p21 and BAX protein levels were determined by western blot analysis. \* $P < .05$  vs pcDNA3.1 group

myocytes, the absence of UT-B could cause mitochondrial dysfunction.<sup>3</sup> Taking these results together, we suggest that moderate UT-B expression is an important condition for cells to maintain mitochondrial function.

Various ROS are harmful byproducts of mitochondrial respiration. The formation of mitochondrial ROS is an important component of cell metabolism and plays an important role in cell physiology.<sup>23</sup> Increased ROS is responsible for the accumulation of ROS-related lesions in DNA, proteins and lipids, which may lead to progressive cell dysfunction, resulting in apoptosis. In our experiment, in B16 cells transfected with pcDNA3.1-UT-B, intracellular ROS was clearly increased; the toxic effect of ROS accumulation may be a cause of death of B16 cells after transfection with pcDNA3.1-UT-B. However, some results suggest that ROS is an important factor in reducing  $\Delta\psi_m$ .<sup>24</sup> After UT-B is overexpressed in B16 cells, mitochondrial dysfunction occurs and ROS production increases; one promotes the other to form a vicious cycle.

Activation of p53 induces cell cycle arrest and apoptosis in cells, rendering some cells resistant to radiotherapy and chemotherapy.<sup>25,26</sup> After transfection with pcDNA3.1-UT-B, the expression of p53 increased, which may have induced apoptosis of B16 cells.

MDM2 binds to p53, preventing it from participating in transcription and inducing its degradation.<sup>27,28</sup> Some groups have begun to develop small molecules that can specifically regulate p53 activity. Small molecule inhibitors such as the analogs of MI-219 and Nutlin-3 inhibit the interaction of MDM2 and p53, releasing wild-type p53 and inducing apoptosis in cancer cells.<sup>29</sup> Our results show that after transfection with pcDNA3.1-UT-B, MDM2 expression was reduced and downstream p21 expression was increased, confirming the activation of p53. In addition, activation of AKT promotes nuclear entry of MDM2, decreases cellular levels of p53, and decreases p53 transcriptional activity, promoting cell survival and cell cycle progression.<sup>30</sup> We detected a decrease in p-AKT expression, further confirming p53 activation after transfection with pcDNA3.1-UT-B.

It has been reported that p53 translocates to the mitochondria and binds to BCL-2 or BCL-XL, thereby allowing BAX to dissociate and oligomerize<sup>31,32</sup> and translocate to the mitochondrial outer membrane. It then causes mitochondrial outer membrane permeabilization, releasing cytochrome C and inducing apoptosis.<sup>33,34</sup> In this study, after transfection of B16 cells with pcDNA3.1-UT-B, cytochrome C was released from mitochondria; downregulated BCL-2 and upregulated BAX levels were related to melanoma cell apoptosis,

presenting further evidence that the p53 pathway is activated when UT-B is overexpressed in B16 cells.

p53 is an important guardian of the genome; its expression is induced by chemical or radiation exposure and other stress conditions.<sup>35</sup> Chowdhury et al reported that mitochondrial functional defects induced *TP53* gene expression when HCT colon cancer cells were treated with respiratory inhibitors.<sup>36</sup> In this experiment, mitochondrial damage induced by overexpression of UT-B may be a result of p53 activation. However, the mechanism by which UT-B overexpression in a UT-B-absent melanoma cell line induces mitochondrial dysfunction and apoptosis requires further study.

This is the first known report to date to describe the role of UT-B protein in skin. We have confirmed the role of UT-B in the development of skin melanoma, and how changes in UT-B function may seriously affect the long-term health of skin. These studies not only contribute to our understanding of skin lesion development but may also improve knowledge of other cancer types. Further research is needed to elucidate the physiological role and mechanism of UT-B in human skin.

## ACKNOWLEDGMENTS

We are grateful to all members of the Pathophysiology Laboratory of the Basic Medical College of Jilin University for their technical support.

## DISCLOSURE

The authors have no conflict of interest.

## ORCID

Yan Meng  <https://orcid.org/0000-0002-7402-9901>

## REFERENCES

- Marzuka A, Huang L, Theodosakis N, Bosenberg M. Melanoma treatments: advances and mechanisms. *J Cell Physiol*. 2015;230:2626-2633.
- Siegel R, Ma J, Zou Z, Jemal A. Cancer statistics, 2014. *CA Cancer J Clin*. 2014;64:9-29.
- Du Y, Meng Y, Zhu J, et al. Quantitative proteomic study of myocardial mitochondria in urea transporter B knockout mice. *Proteomics*. 2014;14:2072-2083.
- Vyas S, Zaganjor E, Haigis MC. Mitochondria and cancer. *Cell*. 2016;166:555-566.
- Tian Y, Qin L, Qiu H, et al. RPS3 regulates melanoma cell growth and apoptosis by targeting Cyto C/Ca2+ /MICU1 dependent mitochondrial signaling. *Oncotarget*. 2015;6:29614-29625.
- Chang YL, Gao HW, Chiang CP, et al. Human mitochondrial NAD(P) (+)-dependent malic enzyme participates in cutaneous melanoma progression and invasion. *J Invest Dermatol*. 2015;135:807-815.
- Li C, Xue H, Lei Y, Zhu J, Yang B, Gai X. Clinical significance of the reduction of UT-B expression in urothelial carcinoma of the bladder. *Pathol Res Pract*. 2014;210:799-803.
- Liu J, Xie L, Yin A. (2013). Expression of urea transporters in sweat gland tissue of normal subjects and uremic patients. *Nan Fang Yi Ke Da Xue Xue Bao*; 33: 951-955.
- Abdollah F, Boorjian S, Cozzarini C, et al. Survival following biochemical recurrence after radical prostatectomy and adjuvant radiotherapy in patients with prostate cancer: the impact of competing causes of mortality and patient stratification. *Eur Urol*. 2013;64:557-564.
- Dong Z, Ran J, Zhou H, et al. Urea transporter UT-B deletion induces DNA damage and apoptosis in mouse bladder urothelium. *PLoS ONE*. 2013;8:e76952.
- Li F, Lei T, Zhu J, et al. A novel small-molecule thienoquinolin urea transporter inhibitor acts as a potential diuretic. *Kidney Int*. 2013;83:1076-1086.
- Laqaes D, Santos A, Grasberger PE, et al. Targeted apoptosis of myofibroblasts with BH3 mimetic ABT-263 reverses established fibrosis. *Sci Transl Med*. 2017;9:eaa13765.
- Zhang Y, Cao W, Toneri M, et al. Toxicology and efficacy of tumor-targeting *Salmonella typhimurium* A1-R compared to VNP 20009 in a syngeneic mouse tumor model in immunocompetent mice. *Oncotarget*. 2017;8:54616-54628.
- Mayer B, Oberbauer R. Mitochondrial regulation of apoptosis. *News Physiol Sci: an international journal of physiology produced jointly by the International Union of Physiological Sciences and the American Physiological Society*. 2003;18:89-94.
- Adams JM, Cory S. The Bcl-2 apoptotic switch in cancer development and therapy. *Oncogene*. 2007;26:1324-1337.
- Youle RJ, Strasser A. The BCL-2 protein family: opposing activities that mediate cell death. *Nat Rev Mol Cell Biol*. 2008;9:47-59.
- Selivanova G. Therapeutic targeting of p53 by small molecules. *Semin Cancer Biol*. 2010;20:46-56.
- Joerger AC, Fersht AR. The tumor suppressor p53: from structures to drug discovery. *Cold Spring Harb Perspect Biol*. 2010;2:a000919.
- Wang W, El-Deiry WS. Restoration of p53 to limit tumor growth. *Curr Opin Oncol*. 2008;20:90-96.
- Zhou BP, Liao Y, Xia W, Zou Y, Spohn B, Hung MC. HER-2/neu induces p53 ubiquitination via Akt-mediated MDM2 phosphorylation. *Nat Cell Biol*. 2001;3:973-982.
- Nagamani SCS, Erezc A. A metabolic link between the urea cycle and cancer cell proliferation. *Mol Cell Oncol*. 2016;3:e1127314.
- Long Y, Tsai WB, Wangpaichitr M, et al. Arginine deiminase resistance in melanoma cells is associated with metabolic reprogramming, glucose dependence, and glutamine addiction. *Mol Cancer Ther*. 2013;12:2581-2590.
- Ying Y, Padanilam BJ. Regulation of necrotic cell death: p53, PARP1 and cyclophilin D-overlapping pathways of regulated necrosis? *Cell Mol Life Sci*. 2016;73:2309-2324.
- Zhang Z, Zhao X, Qin X. Potential genotoxic and cytotoxicity of emamectin benzoate in human normal liver cells. *Oncotarget*. 2017;8:82185-82195.
- Ryan KM, Phillips AC, Vousden KH. Regulation and function of the p53 tumor suppressor protein. *Curr Opin Cell Biol*. 2001;13:332-337.
- Saha MN, Qiu L, Chang H. Targeting p53 by small molecules in hematological malignancies. *J Hematol Oncol*. 2013;6:23.
- Bates S, Vousden KH. Mechanisms of p53-mediated apoptosis. *Cell Mol Life Sci*. 1999;55:28-37.
- Essmann F, Schulze-Osthoff K. Translational approaches targeting the p53 pathway for anti-cancer therapy. *Br J Pharmacol*. 2012;165:328-344.
- Shangary S, Wang S. Small-molecule inhibitors of the MDM2-p53 protein-protein interaction to reactivate p53 function: a novel approach for cancer therapy. *Annu Rev Pharmacol Toxicol*. 2009;49:223-241.
- Mayo LD, Donner DB. A phosphatidylinositol 3-kinase/Akt pathway promotes translocation of Mdm2 from the cytoplasm to the nucleus. *Proc Natl Acad Sci USA*. 2001;98:11598-11603.

31. Mihara M, Erster S, Zaika A, et al. p53 has a direct apoptogenic role at the mitochondria. *Mol Cell*. 2003;11:577-590.
32. Chipuk JE, Kuwana T, Bouchier-Hayes L, et al. Direct activation of Bax by p53 mediates mitochondrial membrane permeabilization and apoptosis. *Science*. 2004;303:1010-1014.
33. Chipuk JE, Green DR. How do BCL-2 proteins induce mitochondrial outer membrane permeabilization? *Trends Cell Biol*. 2008;18:157-164.
34. David R: Apoptosis A lipid trigger of MOMP. *Nat Rev Mol Cell Biol*. 2012;13:208-209.
35. Lowe SW, Ruley HE, Jacks T, Housman DE. p53-dependent apoptosis modulates the cytotoxicity of anticancer agents. *Cell*. 1993;74:957-967.
36. Chowdhury AR, Long A, Fuchs SY, Rustgi A, Avadhani NG. Mitochondrial stress-induced p53 attenuates HIF-1alpha activity by physical association and enhanced ubiquitination. *Oncogene*. 2017;36:397-409.

**How to cite this article:** Liu L, Sun Y, Zhao Y, et al. Urea transport B gene induces melanoma B16 cell death via activation of p53 and mitochondrial apoptosis. *Cancer Sci*. 2018;109:3762-3773. <https://doi.org/10.1111/cas.13825>